THE JOURNAL OF PHYSICAL CHEMISTRY B
A JOURNAL OF THE AMERICAN CHEMICAL SOCIETY

pubs.acs.org/JPCB Article

Effects of Molecular Crowders on Single-Molecule Nucleic Acid Folding: Temperature-Dependent Studies Reveal True Crowding vs Enthalpic Interactions

Hsuan-Lei Sung and David J. Nesbitt*

Cite This: J. Phys. Chem. B 2021, 125, 13147−13157 Read Online

ACCESS | Metrics & More | Article Recommendations

ABSTRACT: Biomolecular folding in cells can be strongly influenced by spatial overlap/excluded volume interactions (i.e., "crowding") with intracellular solutes. As a result, traditional in vitro experiments with dilute buffers may not accurately recapitulate biomolecule folding behavior in vivo. In order to account for such ubiquitous excluded volume effects, biologically inert polyethylene glycol (PEG) and polysaccharides (dextran and Ficoll) are often used as in vitro crowding agents to mimic in vivo crowding conditions, with a common observation that high concentrations of these polymers stabilize the more compact biomolecule conformation. However, such an analysis can be distorted by differences in polymer interactions with the folded vs unfolded conformers, requiring temperature-dependent analysis of the thermodynamics to reliably assess competing enthalpic vs entropic contributions and thus the explicit role of excluded volume. In this work, temperature-controlled single-molecule fluorescence resonance energy transfer (smFRET) is used to characterize the thermodynamic interaction between nucleic acids and common polymer crowders PEG, dextran, and Ficoll. The results reveal that PEG promotes secondary and tertiary nucleic acid folding by simultaneously increasing the folding rate while decreasing the unfolding rate, with temperature-dependent studies confirming that the source of PEG stabilization is predominantly entropic and consistent with a true excluded volume crowding mechanism. By way of contrast, neither dextran nor Ficoll induces any significant concentration-dependent change in nucleic acid folding stability at room temperature, but instead, stabilization effects gradually appear with a temperature increase. Such a thermal response indicates that both folding enthalpies and entropies are impacted by dextran and Ficoll. A detailed thermodynamic analysis of the kinetics suggests that, instead of true entropic molecular crowding, dextran and Ficoll associate preferentially with the unfolded vs folded nucleic acid conformer as a result of larger solvent accessible surface area, thereby skewing the free energy landscapes through both significant entropic/enthalpic contributions that compete and fortuitously cancel near room temperature.

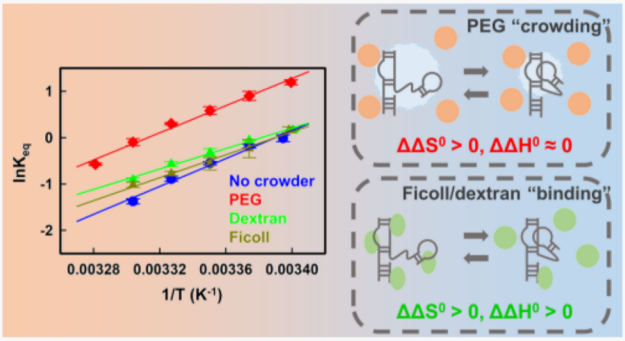

1. INTRODUCTION

The cell is an extremely crowded environment, with 20% of the mass taken up by various organic and biopolymer solutes, such as proteins, nucleic acids, and small molecule metabolites.[1,2] This raises the real likelihood that biomolecules in vivo function differently from the in vitro behavior traditionally observed in biochemical assays under dilute buffer conditions.[3,4] Correct assessment of the impact of each solute species on the biomolecular structure and function is extremely challenging to quantify, particularly under such highly concentrated, nonideal solution conditions. However, these solutes do share one simplifying contribution in common: they all take up physical space in solution and therefore impose fundamental steric constraints on the biomolecule, widely known as excluded volume interactions.[5,6] Simply stated, the presence of excess solute reduces the space available for a specific biomolecule to sample; as a result, the biomolecule is driven into a more compact configuration to maximize the accessible microstates for the overall biomolecule + solvent system.[3] In other words, excluded volume effects are predicted to entropically promote biomolecule folding/compaction, with this critical yet ubiquitous stabilization mechanism commonly referred to as "molecular crowding."[7−9]

Experimentally, the effects of cellular crowding are often studied by adding polymeric macromolecules such as poly-

Received: September 4, 2021
Revised: November 8, 2021
Published: November 23, 2021

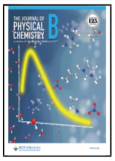

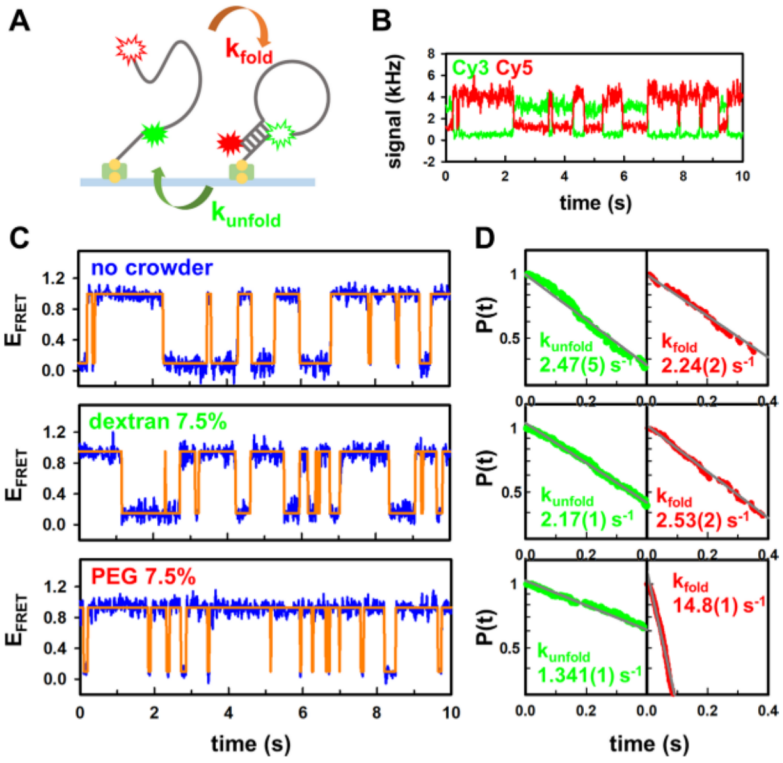

Figure 1. Sample smFRET experiment data. (A) Cartoon depiction of DNA hairpin secondary structure folding and (B) resulting time-resolved single-molecule fluorescent signal from the donor, Cy3 (green), and acceptor, Cy5 (red). (C) Sample time-dependent E_{FRET} trajectories (blue) and the simulated time trace by the simple thresholding method (orange); (D) corresponding dwell time distribution functions of the folded and unfolded conformations with (from top to bottom) 0 wt % crowder, 7.5 wt % dextran, and 7.5 wt % PEG. Data are fit to a single exponential decay function to obtain the rate constants k_{fold}/k_{unfold}, with uncertainties evaluated from the fits.

ethylene glycol (PEG) or polysaccharides such as dextran and Ficoll into the buffers.[9−12] Such polymers have been shown to resist protein adhesion and are believed to be biologically inert.[13,14] They are thus often referred to as "crowders" due to the possible predominance of these excluded volume (entropic) effects over other (enthalpic) chemical interactions.[15−17] Indeed, in the presence of these crowders, enhanced biomolecular folding has often been observed, qualitatively consistent with predictions of excluded volume energetically favoring the more compact state.[18] Furthermore, early temperature-dependent studies of dextran stabilized lysozyme folding have revealed that the melting transition temperatures (T_m) increase predominantly due to entropic interactions with dextran and yet with essentially negligible enthalpic contributions.[16] It is this predominance of entropic stabilization that is a robust and distinctive feature of the excluded volume mechanism and the resulting molecular crowding effects. Identification of crowding effects arising solely through entropic contributions with inert polymers has since been demonstrated for both proteins and nucleic acids, requiring detailed thermodynamic investigations as a function of temperature.[16,17,19−21]

In intriguing contrast with these early crowding studies, more recent results have suggested that both PEG and polysaccharide crowders may also influence the net folding enthalpies for certain protein systems.[22−25] Indeed, it is not particularly surprising that such molecules could exhibit differential chemical interactions with folded vs unfolded biomolecules above and beyond simple excluded volume interactions. These studies highlight the simple fact that chemical interactions can depend significantly on both structure/charge states of the biomolecule and the presence of specific moieties on the crowding polymer species.[19] It is worth noting that most of these previous thermodynamic studies have focused on folding/unfolding in proteins, with characterization of the corresponding molecular crowding effects with nucleic acids still very much in its infancy.[26−28]

To address this informational lacuna, we explore herein the effects of the most commonly used polymeric molecular crowders (i.e., PEG, dextran, and Ficoll) on both secondary and tertiary structures of nucleic acid constructs by temperature-controlled single-molecule FRET spectroscopy (smFRET).[29,30] In this work, the folding/unfolding equilibria and kinetics are revealed at the single-molecule level, with deconstruction of free energies into enthalpic and entropic components extracted from temperature-dependent crowding studies. The studies indeed reveal PEG stabilization of nucleic acid folded structures to be predominantly entropic, consistent with the simple picture of pure crowding dynamics originating from excluded volume effects.[16,17] More surprisingly, we find that the commonly used polysaccharide crowders dextran and Ficoll do not significantly impact either folding/unfolding kinetics or thermodynamic stability of nucleic acids, at least at room temperature. Interestingly, however, temperature-dependent studies reveal this lack of crowding impact to be due to accidental cancellation between folding enthalpy (ΔH) and entropy ($-T\Delta S$) contributions at room temperature, where additional changes in the enthalpy result from the preferential binding of the polysaccharide molecules to the more solvent-exposed unfolded conformation of the nucleic acid.

https://doi.org/10.1021/acs.jpcb.1c07852
J. Phys. Chem. B 2021, 125, 13147−13157

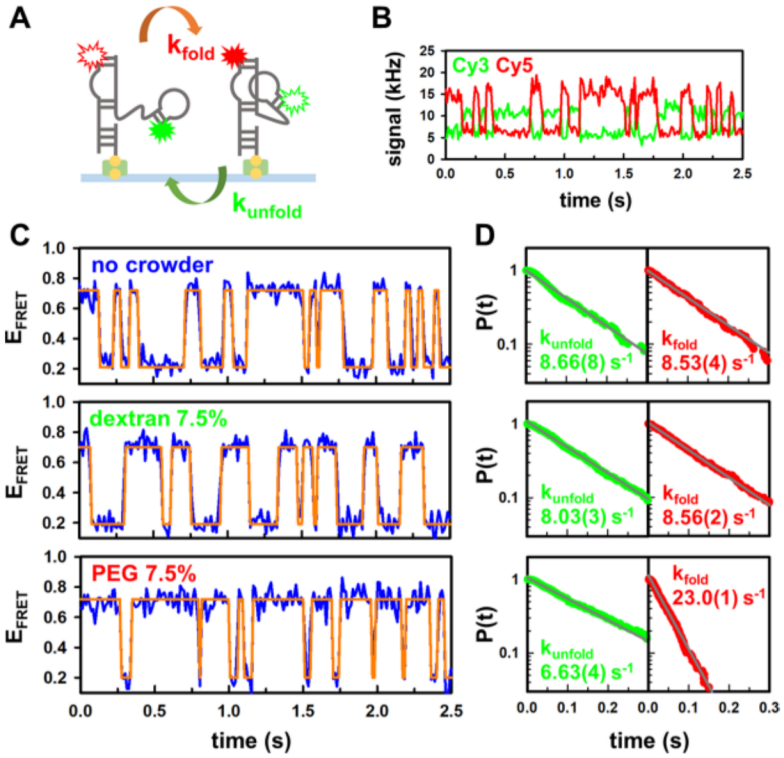

Figure 2. Sample smFRET experiment data. (A) Cartoon depiction of TL-TLR tertiary structure folding and (B) resulting time-resolved single-molecule fluorescent signal from the donor, Cy3 (green), and acceptor, Cy5 (red). (C) Sample time-dependent E_{FRET} trajectories (blue) and the simulated time trace by the simple thresholding method (orange); (D) corresponding dwell time distribution functions of the folded and unfolded conformations with (from top to bottom) 0 wt % crowder, 7.5 wt % dextran, and 7.5 wt % PEG. Data are fit to a single exponential decay function to obtain the rate constants k_{fold}/k_{unfold}, with uncertainties evaluated from the fits.

2. EXPERIMENTAL SECTION

2.1. Nucleic Acid Constructs and Sample Preparation. In order to study molecular crowding interaction on nucleic acids as a function of secondary vs tertiary structure, we exploit a simple DNA hairpin (Figure 1) and the ubiquitous RNA tetraloop−tetraloop receptor tertiary folding domain (TL-TLR, Figure 2) as model systems, respectively. The DNA hairpin (with a 7 complimentary base pair stem and a 40 dA linker, see Figure 1A) is doubly dye-labeled (Cy3; Cy5), biotinylated for binding to a cover slip surface, purchased in high-performance liquid chromatography (HPLC)-purified form (Integrated DNA technologies, Coralville, IA), and used as is.[31,32] The ternary TL-TLR construct comprises three smaller oligonucleotides, each singly labeled with Cy3, Cy5, or biotin (Integrated DNA technologies, Coralville, IA), as described in detail elsewhere.[33] The full ternary construct is then prepared by heat-annealing the three oligomers together followed by purification via HPLC.

The smFRET sample preparation is achieved by first coating the surface of a standard glass coverslip with an excess bovine serum albumin (BSA) and biotinylated BSA mixture followed by incubation with streptavidin solution to generate a streptavidin-decorated surface. The resulting secondary and tertiary nucleic acid constructs are then immobilized on the surface of the coverslip through the highly stable biotin−streptavidin interactions, which permits prolonged observation of the folding/unfolding kinetics under conditions over several minutes to fractions of an hour. The smFRET imaging buffer consists of (i) 50 mM HEPES-KOH buffer (pH = 7.5), (ii) NaCl to provide background monovalent cation concentrations of $[M^+]$ = 100 or 150 mM for hairpin or TL-TLR constructs, respectively, (iii) an enzymatic oxygen scavenger cocktail (PCD/PCA/Trolox) to increase fluorophore photostability,[34] and (iv) polymeric crowders PEG 6 k, dextran 6 k (M_W = 6000 amu), or Ficoll PM70 (MW = 70,000 amu) to achieve the desired concentration conditions (0−10 wt %), chosen to allow reliable extraction of rate constants (k_{fold} and k_{unfold}) within the limits of our experimental time resolution (see Section 2.3).

2.2. Single-Molecule FRET Spectroscopy and Temperature Control. The smFRET experiment in this work is performed with a home-built confocal microscope system,[35] based on a pulsed 532 nm Nd:YAG laser, collimated, and directed onto the sample through an inverted confocal microscope. The beam is tightly focused into a diffraction limited spot by a 1.2 N.A. water immersion objective, achieving $\lambda/(2NA) \approx 220$ nm spatial resolution and allowing observation of one fluorophore-labeled construct at a time. The resulting emitted signal fluorescence is then collected through the same objective, with photons split into four different channels corresponding to red vs green, horizontal vs vertical polarizations before detection on four separate avalanche photodiodes. For each detected photon, four bits of information, color, polarization, wall-clock time (in 50 ns bins), and microtime (with respect to the laser pulse and with 50 ps resolution), are recorded with fast time to amplitude conversion and/or time-correlated single-photon counting modules. In this work, we average over polarization effects by simply grouping all green (donor Cy3) and red (acceptor Cy5) photons to calculate FRET efficiency (E_{FRET}) as a

https://doi.org/10.1021/acs.jpcb.1c07852
J. Phys. Chem. B 2021, 125, 13147−13157

function of time and thereby obtain the resulting E_{FRET} trajectories.

To achieve precise temperature control, the sample and the microscope objective are heated simultaneously to minimize thermal gradients.[36,37] Specifically, the sample holder is mounted to a thermal stage (Instec, Boulder, CO), which regulates the sample temperature by servo loop-controlled heating and cooling. At the same time, the objective is heated using a commercially available resistive collar (Bioptechs, Butler, PA). Prior to each experiment, a 15 min incubation time allows the sample to achieve a steady temperature (± 0.1 °C).

2.3. Single-Molecule FRET Data Analysis. We calculate the background and cross-talk corrected FRET energy transfer efficiency E_{FRET} ($E_{FRET} = I_A / (I_D + I_A)$) at 10 ms bin time resolution to generate the time-dependent E_{FRET} trajectories. Due to widely separated E_{FRET} values for folded (high E_{FRET}) and unfolded (low E_{FRET}) conformations (Figure 1C and 2C), a simple thresholding routine is adopted to determine the folding/unfolding states as well as the corresponding dwell time distributions.[35,38] The folding equilibrium constant K_{eq} can be readily obtained by the ratios of total dwell times for the folded and unfolded states. Furthermore, our kinetic analysis is achieved by generating cumulative distribution functions of the dwell times for each state (see Figures 1D and 2D for sample data). For both constructs, the resulting folded/unfolded dwell time distributions P(t) are well fit to single exponential decay functions to extract rate constants k_{unfold}/k_{fold}, respectively, confirming that the folding/unfolding processes can be satisfactorily characterized by first-order kinetics.[39]

3. RESULTS AND ANALYSIS

3.1. Crowder Effects on the DNA Hairpin Secondary Folding Kinetics. Folding of the 7-base pair DNA hairpin involves formation of secondary double helix structure essential for nucleic acid function. Its unimolecular design simplicity and easily tunable folding/unfolding rates make this an ideal model system for exploring nucleic acid secondary folding through single-molecule kinetic studies (Figure 1A).[38,40,41] Herein, we explore the effects of three polymer crowders widely used in crowding studies: PEG, dextran, and Ficoll. These species have been consistently shown to stabilize the folded conformation of biomolecules,[9−12] primarily proteins, although the thermodynamic origin of this stabilization still remains debatable and probably structure-dependent.[19]

In the absence of crowders, the secondary folding equilibria of the DNA hairpin construct are adjusted by NaCl in the buffer to achieve $K_{eq} \approx 1$ conditions (at room temperature 21.0 ± 0.2 °C), in order to permit the maximum dynamic range in ΔK_{eq} for shifts in either the folded or unfolded directions (Figure 1). In the presence of PEG (M_W = 6000 amu), the folding equilibrium K_{eq} is greatly enhanced, with a nearly 20-fold increase at the maximal PEG concentrations (10% by weight, or 10 wt %) in this study (Figure 3A). Conversely, both polysaccharide crowders clearly exhibit much smaller effects, with only a 20 and 50% increase in K_{eq} for 10 wt % dextran (M_W = 6000 amu) and Ficoll (M_W = 70,000 amu), respectively. Furthermore, complementary kinetic information on folding/unfolding rate constants can be obtained by dwell time analysis of the single-molecule E_{FRET} trajectories (Figure 1C,D). As clearly evident in Figure 3, PEG promotes the DNA hairpin folding by simultaneously increasing k_{fold} and decreasing k_{unfold}. Indeed, this effect is particularly significant for k_{fold}, which exhibits an order of magnitude increase at 10 wt % PEG, with a relatively smaller but still quite noticeable twofold reduction observed for k_{unfold}. By way of contrast, similar wt % concentrations of the polysaccharide dextran and Ficoll increase k_{fold}, by a relatively small amount (<60%), with only negligible effects on k_{unfold} (<10%) within experimental uncertainty.

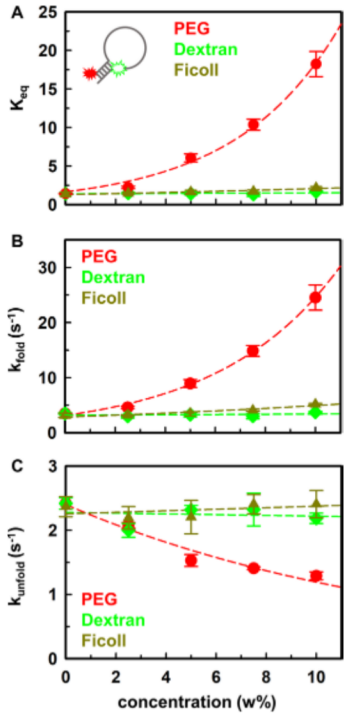

Figure 3. Crowder effects on DNA hairpin folding at constant room temperature (21 °C). Crowder concentration dependence of (A) K_{eq}, (B) k_{fold}, and (C) k_{unfold}. Error bars represent standard deviation of the mean (N = 3). Data are fit to a single exponential function based on the empirical observation of solute effects on the free energy change upon folding (see the text for more details).

3.2. Crowder Effects on the RNA TL-TLR Tertiary Folding Kinetics. TL-TLR is a ubiquitous folding element that is widely found in RNA tertiary structures (Figure 2A).[42] It has been extensively studied at the single-molecule level,[33] and its kinetic/thermodynamic responses to PEG are found to be consistent with crowding effects reported in previous studies.[17,43] Again by way of contrast, the potential crowding effects of dextran and Ficoll on such a common tertiary RNA folding motif have remained largely unexplored.

As a function of increasing concentration, PEG significantly promotes TL-TLR folding, with a more than sixfold increase in K_{eq} at 10 wt %, whereas dextran and Ficoll induce only much smaller increases in K_{eq} (<50%, Figure 4A), very much consistent with the DNA hairpin results. Furthermore, kinetic analysis of the smFRET trajectories indicates k_{fold} for the TL-TLR to increase exponentially with PEG concentration, but it remains surprisingly constant (<20%) in response to dextran and Ficoll (Figure 4B). Interestingly, k_{unfold} for the TL-TLR construct is reduced comparably by all three crowders (Figure 4C), although the impact of PEG crowding is still the largest. It is also worth noting that the putative crowding dependences of K_{eq} and k_{fold}/k_{unfod} are well fit (dashed lines in Figures 3 and 4) to exponential growth/decay functions, which would be

https://doi.org/10.1021/acs.jpcb.1c07852
J. Phys. Chem. B 2021, 125, 13147−13157

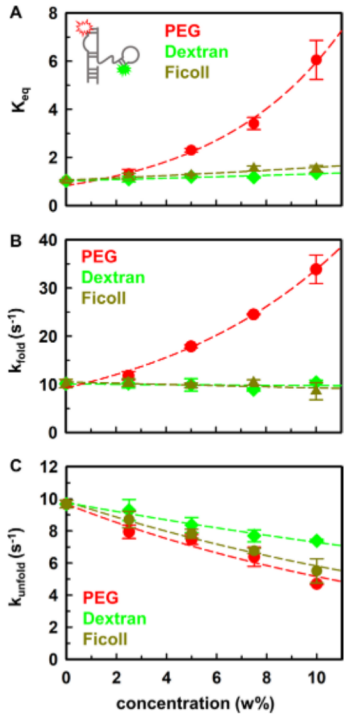

Figure 4. Crowder effects on RNA TL-TLR folding at constant room temperature (21 °C). Crowder concentration dependence of (A) K_{eq}, (B) k_{fold}, and (C) k_{unfold}. Error bars represent standard deviation of the mean (N = 3). Data are fit to a single exponential function based on the empirical observation of solute effects on the free energy change upon folding (see the text for details).

entirely consistent with empirically observed linear relationships between folding free energy changes ($\Delta\Delta G$) and solute concentration.[44,45] Specifically, the strength of the solute interaction is often characterized by the so-called m-value,[46−48] which corresponds to exponents in exponential growth/decay fits of the concentration-dependent K_{eq} in Figure 3A and 4A. In the interest of completeness, the corresponding m-values of the crowder-TL-TLR interaction can be least squares fitted and found to be −0.115(6), −0.015(2), and −0.023(4) kcal mol^{-1} wt %$^{-1}$ for PEG, dextran, and Ficoll, respectively. The m-value from PEG concentration dependence is therefore >5 times larger than that from dextran/Ficoll, again highlighting the fact that the TL-TLR folding free energy is much more sensitive to PEG crowding. A similar crowder concentration dependence is also observed for the DNA hairpin, with m-values for PEG, dextran, and Ficoll determined to be −0.141(8), −0.005(6), and −0.027(4) kcal mol^{-1} wt %$^{-1}$, respectively.

Our results indicate that PEG promotes both nucleic acid secondary and tertiary folding by simultaneously increasing k_{fold} and decreasing k_{unfold}. However, the polysaccharide crowders dextran and Ficoll show little to no effect on both nucleic acid folding equilibria and kinetics, i.e., corresponding to $\Delta\Delta G \approx 0$. This is already substantially different from results of several previous protein folding studies, where the prominent stabilization effects were observed and often attributed to crowding.[5] It is worth noting that the above differential results for the impact of dextran or Ficoll on nucleic acid folding could reflect two quite different scenarios. It could be that there is vanishingly small differential interaction enthalpy ($\Delta\Delta H^0 \approx 0$) between the solutes and the folded or unfolded biomolecule in which case the observed $\Delta\Delta G^0 \approx 0$ would translate into $\Delta\Delta S^0 \approx 0$ and therefore no entropic crowding. However, $\Delta\Delta G^0 \approx 0$ could also reflect the coincidental balance between competing enthalpic and entropic contributions at a single temperature. Thus, an unambiguous determination of whether dextran and Ficoll have only minimal differential interactions with our folded/unfolded nucleic acid constructs requires additional van't Hoff and Arrhenius investigation of the temperature-dependent equilibrium and kinetic behavior, as described below.

3.3. Crowding Effects on DNA Secondary Structure Folding Thermodynamics. Conventional modeling of "pure" molecular crowding dynamics based on hard sphere excluded volume considerations explicitly ignores any chemical interactions between the crowder and the crowded species. As a result, such crowding dynamics automatically satisfy $\Delta(\Delta H^0) \approx 0$ (where the second Δ reflects the differential presence/absence of crowders) and should ideally contribute only entropically ($\Delta\Delta S^0 > 0$) to the overall folding free energy.[5,17,19] Herein, we explore the temperature-dependent response of nucleic acid folding to identify the thermodynamics of the solute−biomolecule crowder interactions. Specifically, van't Hoff analysis allows deconstruction of the folding free energies into entropic and enthalpic components via

$$\ln(K_{eq}) = -\frac{\Delta G^0}{RT} = -\frac{\Delta H^0}{R}\frac{1}{T} + \frac{\Delta S^0}{R} \quad (1)$$

From a standard $\ln(K_{eq})$ vs $1/T$ van't Hoff plot (e.g., see Figure 5), the slope and intercept permit independent

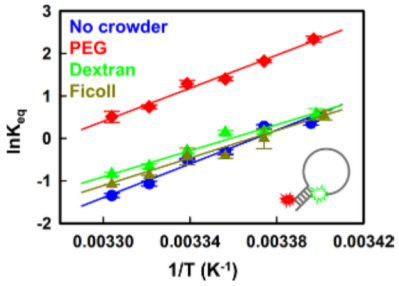

Figure 5. van't Hoff plot for the temperature-dependent K_{eq} of the DNA hairpin construct at constant crowder concentrations (0 or 7.5 wt %). Least squares fits of the data to eq 1 yield changes in overall enthalpies (ΔH^0) and entropies (ΔS^0).

quantitation of enthalpic ($-\Delta H^0/R$) and entropic ($\Delta S^0/R$) changes upon folding, respectively, which can be studied in the absence/presence of crowding agents.

In the absence of crowders, the DNA hairpin becomes less stable and unfolds with increasing temperature, consistent with temperature-induced melting/denaturation routinely observed for nucleic acid secondary structure.[49] Moreover, the linear van't Hoff plot reveals a positive slope and a negative intercept (Figure 5), corresponding to negative folding enthalpy ($\Delta H^0 < 0$) and entropy ($\Delta S^0 < 0$) changes, respectively. Such free energy behavior agrees with the common physical picture of folding where biomolecules are enthalpically driven into the more order folded conformation.[33,50] The presence of PEG vertically translates the linear fit upward with respect to zero-crowder conditions, suggesting a decrease in entropic penalty ($\Delta\Delta S^0 > 0$) with essentially unchanged enthalpic gain ($\Delta\Delta H^0 \approx 0$). Such predominantly entropic stabilization is of course

https://doi.org/10.1021/acs.jpcb.1c07852
J. Phys. Chem. B 2021, 125, 13147−13157

consistent with crowding effects resulting from excluded volume.[5,17,19] By way of contrast, dextran and Ficoll clearly reveal a more complex temperature-dependent behavior, with a decrease in the slopes ($\Delta\Delta H^0 > 0$) and increase in the intercepts ($\Delta\Delta S^0 > 0$). Such nonzero enthalpic contributions clearly signal additional solute-specific chemical interactions and changes in these interactions as a function of crowding environments.

In addition to these equilibrium results for K_{eq}, the folding rate constants k_{fold} and k_{unfold} also depend on temperature and contain equally valuable thermodynamic information. For secondary structure in the DNA hairpin, the data reveal a dramatic increase in both k_{fold} and k_{unfold} rate constants at elevated temperature (see Figure 6), signaling a significantly

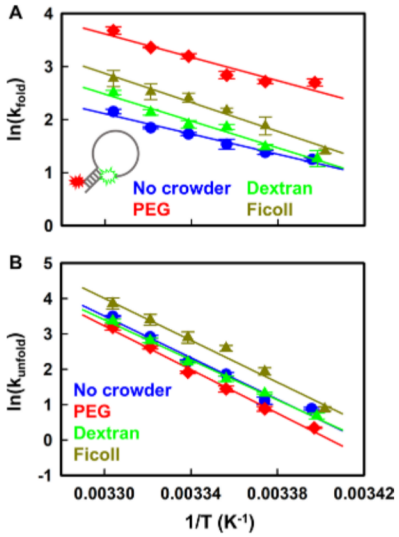

Figure 6. Eyring plot for the temperature-dependent (A) k_{fold} and (B) k_{unfold} of the DNA hairpin construct at constant crowder concentrations (0 or 7.5 wt %). Least squares fits of the data to eq 2 yield forward/reverse activation enthalpies ($\Delta H^{\ddagger}$) and entropies ($\Delta S^{\ddagger}$) for k_{fold}/k_{unfold}.

endothermic approach to the transition state from both folded/unfolded sides of the barrier. Based on results from other single-molecule studies,[51] such an enthalpic penalty likely arises from competition between Coulomb repulsion of the negatively charged DNA strands and the lack of complete hydrogen bond formation in the transition state. The corresponding entropy changes can be obtained from Eyring analysis of the temperature-dependent k_{fold}/k_{unfold} with the transition state expression:[52]

$$\ln(k) = -\frac{\Delta H^{\ddagger}}{R}\frac{1}{T} + \frac{\Delta S^{\ddagger}}{R} + \ln \nu \qquad (2)$$

where ν represents the attempt frequency sampling the free energy barrier along the folding coordinate. From such a standard Eyring plot of lnk vs $1/T$ (see Figure 6), the slopes and intercepts for ln k_{fold} or ln k_{unfold} correspond to the activation enthalpy ($-\Delta H^{\ddagger}/R$) and entropy ($\Delta S^{\ddagger}/R + \ln\nu$) from either the folded (F) or the unfolded (U) state, respectively. Since $\Delta S^{\ddagger}$ depends only weakly (logarithmically) on ν, it suffices in this work to simply estimate ν as a low frequency skeletal vibration with $\nu = 10^{13}$ s^{-1}.[29,53] However, it is also worth noting that any reported changes in the activation entropy (i.e., $\Delta\Delta S^{\ddagger}$) are rigorously independent of this estimate for ν.

For the DNA hairpin, the presence or absence of PEG (red vs blue solid line, Figure 6) does not change the slopes in plots of both k_{fold} and k_{unfold}, with vertical shifts again signaling that PEG promotes secondary nucleic acid folding predominantly through "pure" crowding (i.e., entropic) effects. Furthermore, both the magnitude and sign of these uniform vertical displacements in ln k_{fold} vs ln k_{unfold} are consistent with the PEG-dependent enhancement of folding stability observed at room temperature (Figure 2B,C). The polysaccharide crowders dextran and Ficoll, on the other hand, exhibit more complex behaviors, with the data now revealing significant changes in both slopes ($\Delta\Delta H^{\ddagger} > 0$) and intercepts ($\Delta\Delta S^{\ddagger} > 0$) in the Eyring plots for k_{fold}. Interestingly, however, these slope differences are much less evident for the unfolding step, which is consistent with polysaccharide solute effects primarily influencing the approach to the transition state from the unfolded conformation. Thermodynamic values (ΔH^0, ΔS^0, $\Delta H^{\ddagger}$, and $\Delta S^{\ddagger}$) extracted from these plots for both PEG and polysaccharide solutes are quantitatively summarized in Table 1.

3.4. Crowding Effects on RNA TL-TLR Tertiary Folding Thermodynamics. As for many compact nucleic acid conformations, the TL-TLR tertiary binding motif weakens and unfolds with increasing temperature,[33] with the positive (negative) slope (intercept) in the van't Hoff plot (see Figure 7) indicating folding to be exothermically favored ($\Delta H^0 < 0$)

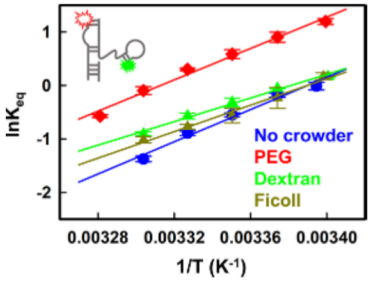

Figure 7. van't Hoff plot for the temperature-dependent K_{eq} of the RNA TL-TLR construct at constant crowder concentrations (0 or 7.5 wt %). Least squares fits of the data to eq 1 yield changes in overall enthalpies (ΔH^0) and entropies (ΔS^0).

Table 1. Thermodynamic Parameters of DNA Hairpin Folding Obtained from van't Hoff and Eyring Analyses[a]

	ΔH^0 (kcal/mol)	ΔH^{0*} (kcal/mol)	ΔS^{0*} (cal/mol/K)	$\Delta H^{\ddagger}$ (kcal/mol)	$\Delta H^{\ddagger*}$ (kcal/mol)	$\Delta S^{\ddagger*}$ (cal/mol/K)
no crowder	−40 (3)	−40.1 (0.9)	−135 (2)	19.1 (1.5)	20.3 (0.6)	11 (2)
7.5 wt % PEG	−39.7 (1.8)	−40.1 (0.9)	−131 (2)	21 (2)	20.3 (0.6)	16 (2)
7.5 wt % dextran	−31 (2)		−103 (9)	25 (2)		29 (7)
7.5 wt % Ficoll	−32 (2)		−109 (7)	27.2 (1.8)		36 (5)

[a]Asterisk (*) indicates results from global fits assuming a common slope (i.e., enthalpy change) between no crowder and 7.5 wt % PEG data.

https://doi.org/10.1021/acs.jpcb.1c07852
J. Phys. Chem. B 2021, 125, 13147−13157

and entropically penalized ($\Delta S^0 < 0$). Once again, the presence of PEG solute at high wt % shifts the linear fits vertically upward without appreciable change in slope ($\Delta\Delta H^0 \approx 0$), which corresponds to a positive change in the intercept ($\Delta\Delta S^0 > 0$). In other words, PEG entropically stabilizes the TL-TLR tertiary structure formation, consistent with a conventional excluded volume mechanism for molecular crowding.[17,43] By way of contrast, the putative polysaccharide "crowders" dextran and Ficoll exhibit decreased slopes and increased intercepts in the van't Hoff plots, indicating significant solute-dependent differential enthalpic interactions, in addition to possible entropic crowding corresponding to a less exothermic ($\Delta\Delta H^0 > 0$) but more entropically favored ($\Delta\Delta S^0 > 0$) folding into the TL-TLR tertiary structure. It is particularly noteworthy that the absence of polysaccharide "crowding" effects observed near room temperature for both the DNA hairpin and RNA TL-TLR constructs (Figures 3 and 4) is simply due to a fortuitous balance between entropic and enthalpic contributions. Indeed, the data in Figure 7 reveal that dextran and Ficoll at 7.5 wt % can and do efficiently stabilize nucleic acid folding at higher (and presumably destabilize at lower) temperatures but only via a temperature-dependent imbalance in enthalpic and entropic contributions to the free energies. Such stabilization effects can be quite comparable to (and indeed easily mistaken for) pure entropic crowding if the temperature dependence is not also carefully explored and taken into account.

The temperature-dependent kinetic data for k_{fold} and k_{unfold} again reiterate the predominantly entropic role of PEG stabilization in RNA tertiary folding, as indicated by parallel vertical shifts in the Eyring plots (Figure 8). Again, by way of contrast, dextran and Ficoll polysaccharides both show quite strong enthalpic and entropic effects on k_{fold}. Indeed, the Eyring plot slopes in Figure 8A for tertiary structure folding even change sign (from plus to minus), indicating that the presence of dextran and Ficoll transforms a normally exothermic prefolding approach into a significantly endothermic approach to the transition state ($\Delta H^{\ddagger} > 0$). Conversely, the temperature dependence of k_{unfold} (Figure 8B) for the TL-TLR construct is much less dramatic. Similar to the effects seen in k_{unfold} for secondary DNA hairpin structure, the presence/absence of polysaccharide solutes for the TL-TLR generates much more subtle changes in the unfolding endothermicity during the U to TS transition. The list of parameters obtained from kinetic/thermodynamic analysis of the PEG vs polysaccharide solute dependence for tertiary TL-TLR folding/unfolding is summarized in Table 2.

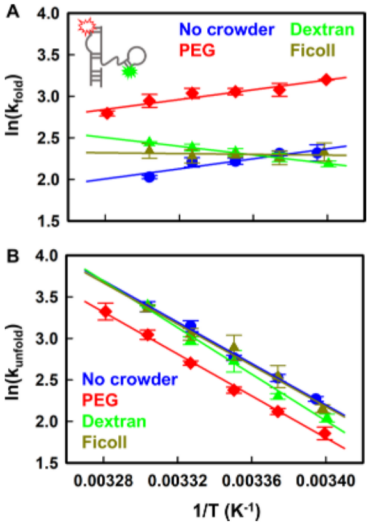

Figure 8. Eyring plots for the temperature-dependent (A) k_{fold} and (B) k_{unfold} of the RNA TL-TLR construct at constant crowder concentrations (0 or 7.5 wt %). Least squares fits of the data to eq 2 yield forward/reverse activation enthalpies ($\Delta H^{\ddagger}$) and entropies ($\Delta S^{\ddagger}$) for k_{fold}/k_{unfold}.

4. DISCUSSION

4.1. Crowder Effects on Nucleic Acid Folding Kinetics. Crowders (or any solute) take up physical space in solution, reducing the volume and the corresponding number of microstates available for a nominally crowded biomolecule to sample.[3] For the same crowder/solute configuration, folded biomolecules (V_F) can generally sample more space than a noncompact unfolded (V_U) structure, where $V_U > V_F$;[2] thus, the presence of solute crowders entropically favors the more compact state of the biomolecule.[21] Furthermore, if the transition state is considered as a partially folded conformation, we can further expect that $V_U > V_{TS} > V_F$. The crowding effect will favor the more compact TS state over U, thereby entropically lowering the free energy barrier for the U to TS transition and consequently increasing k_{fold}.[43] Similarly, k_{unfold} would be expected to decrease with added solute due to the compact F state being more efficiently stabilized by crowding with respect to the TS. In summary, molecular crowding is predicted to promote folding entropically by simultaneously increasing k_{fold} and decreasing k_{unfold}, which is entirely consistent with the PEG data for exponential enhancement of secondary and tertiary structure formation in nucleic acids (see Figures 3 and 4). By way of contrast, polysaccharides dextran and Ficoll at similar wt % concentrations exhibit only quite modest effects on the folding/unfolding rate constants and equilibrium constants ($K_{eq} = k_{fold}/k_{unfold}$) for both the DNA hairpin and the RNA TL-TLR at room temperature. With respect to impact on nucleic acid folding/unfolding dynamics, the single-molecule equilibrium/kinetic data reported herein indicate significant differential enthalpic interactions ($\Delta\Delta H \neq 0$) between the putative polysaccharide "crowders" dextran and Ficoll with nucleic acid constructs. We would argue that such a behavior is inconsistent with conventional excluded volume model predictions, and thus dextran and Ficoll polysaccharides do not represent initiators of molecular crowding phenomena for nucleic acids. Of course, this assessment depends on the nature of chemical interaction with the biomolecule being crowded. We cannot rule out the possibility that dextran and Ficoll have negligible differential chemical interactions between folded vs unfolded proteins and therefore may act as truly entropic crowding agents.[16]

4.2. Predominantly Entropic Effects of PEG Are Consistent with Pure Crowding. Despite the fact that excluded volume effects are ubiquitous for all solutes, the resulting crowding can be buried in or dominated by additional solute- and/or biomolecule-specific enthalpic chemical interactions. The chemically and biologically inactive polymer PEG provides a valuable opportunity for us to identify and isolate pure crowding effects from these other more complex solute−biomolecule interactions. The literature on this important topic is still evolving. To date, many studies have used PEG as the crowding agent and simply report the additional

https://doi.org/10.1021/acs.jpcb.1c07852
J. Phys. Chem. B 2021, 125, 13147−13157

Table 2. Thermodynamic Parameters of RNA TL-TLR Folding Obtained from van't Hoff and Eyring Analyses[a]

	ΔH^0 (kcal/mol)	ΔH^{0*} (kcal/mol)	ΔS^{0*} (cal/mol/K)	$\Delta H^{\ddagger}$ (kcal/mol)	$\Delta H^{\ddagger*}$ (kcal/mol)	$\Delta S^{\ddagger*}$ (cal/mol/K)
no crowder	−30 (2)	−29.5 (1.2)	−101 (4)	−6.0 (1.3)	−5.9 (0.7)	−75 (2)
7.5 wt % PEG	−29.2 (1.6)	−29.5 (1.2)	−97 (3)	−5.9 (0.9)	−5.9 (0.7)	−72 (2)
7.5 wt % dextran	−21.9 (1.2)		−74 (3)	5.17 (0.11)		−37.6 (0.3)
7.5 wt % Ficoll	−24.6 (1.7)		−83 (5)	0.5 (1.0)		−53 (3)

[a]Asterisk (*) indicates results from global fits assuming a common slope (i.e., enthalpy change) between no crowder and 7.5 wt % PEG data.

stabilization to be the result of crowding.[10,40,54,55] However, PEG has also been found to perturb folding enthalpies of some protein systems, implying the presence of solute-specific chemical interactions.[24,25] This differs yet again with multiple other studies on proteins[21] and nucleic acids,[17,20] claiming the effects of PEG to be primarily entropic and therefore reflect true crowding phenomena. Such a discrepancy would seem to indicate that crowding by PEG may depend significantly on the structure and chemical properties of the crowded biomolecules. This provides us with additional motivation for detailed characterization of the thermodynamic crowding effects of PEG, as applied to both secondary and tertiary structures of nucleic acids.

From the temperature-dependent studies reported herein (Figures 5−8), we are able to deconstruct the folding free energy landscape into enthalpic and entropic contributions. Vertical shifts in the van't Hoff plots confirm that PEG only changes the folding entropy ($\Delta\Delta S^0 > 0$) and leaves the enthalpy unchanged ($\Delta\Delta H^0 \approx 0$) for both nucleic acid secondary (Figure 5) and tertiary (Figure 7) folding. The predominantly entropic stabilization effects of PEG are consistent with crowding originating from excluded volume interactions. Furthermore, from transition state analysis, the parallel nature of the Eyring plots for both k_{fold} and k_{unfold} again signals the predominantly entropic origins of PEG stabilization effects (Figures 6 and 8). It is worth noting that our ability to infer small enthalpic changes in these thermodynamic studies is limited by experimental uncertainties. We therefore cannot completely rule out the possibility of small interactions with PEG that could either weakly stabilize or destabilize the nucleic acid. Nevertheless, from previous work on RNA TL-TLR folding, the magnitude of such entropic effects[17] and their dependence on PEG polymer size[43] were successfully predicted by hard sphere models based purely on excluded volume interactions. Strengthened by additional confirming evidence for both nucleic acid secondary and tertiary folding from the temperature-dependent kinetic studies, the data strongly suggest that the PEG crowding of nucleic acids can be largely attributed to true entropic crowding effects.

4.3. Enthalpic/Entropic Effects with Polysaccharides Suggest Preferential Binding. Polysaccharide crowders such as dextran and Ficoll are also commonly used in crowding studies but primarily with proteins.[12] One early study found that lysozyme stability is entropically enhanced by the presence of dextran,[16] from which it was inferred that the effects on protein folding arose primarily from crowding. However, some recent studies have pointed out the additional presence of enthalpic interactions between dextran and Ficoll with certain protein structures.[22,23,56,57] This raises obvious questions about the role of such polysaccharides in the crowding of nucleic acid folding, which has received much less attention and remains poorly understood. This further motivates us to characterize the thermodynamic free energies, enthalpies, and entropies between model secondary and tertiary nucleic acid structure constructs and polysaccharides widely used in protein crowding studies, i.e., dextran and Ficoll.

For both secondary (DNA hairpin) and tertiary (RNA TL-TLR) nucleic acid structures, polysaccharide crowders dextran and Ficoll are found to significantly change enthalpic as well as the entropic contributions to the folding free energy landscape. From standard van't Hoff analysis (Figures 5 and 7), an increase in dextran and Ficoll concentration (0−7.5 wt %) decreases the slope, indicating a reduction in overall exothermicity for folding ($\Delta\Delta H^0 > 0$) but with a corresponding increase in the intercept reflecting a reduction in entropic penalty ($\Delta\Delta S^0 > 0$). Moreover, from temperature-dependent analysis (Figures 6 and 8), we find the effects of these polysaccharides on the folding kinetics to be primarily visible in the folding rate constant k_{fold}. Specifically, dextran and Ficoll are found to increase the folding activation enthalpy ($\Delta\Delta H^{\ddagger} > 0$) and the activation entropy ($\Delta\Delta S^{\ddagger} > 0$) during the approach from U to TS.

The overall folding free energy landscapes and the corresponding crowder-induced changes in the folding/activation enthalpies/entropies are conveniently summarized in Figures 9 and 10 for the secondary (DNA hairpin) and tertiary (RNA TL-TLR) structures, respectively. It is worth noting that along the folding coordinate, the enthalpic penalty ($\Delta\Delta H > 0$) is significant but competes with (and indeed, at room temperature, is completely compensated by) a counterbalancing entropic stabilization ($\Delta(-T\Delta S) < 0$) (Figure 9A,B; Figure 10A,B), leading to a greatly reduced sensitivity in the folding kinetics and equilibrium to both dextran and Ficoll, at least at room temperature where all three Eyring and van't Hoff curves intersect at a single point. Such compensating tradeoffs in free energy between enthalpy and entropy[58] are of course quite ubiquitous in biophysics but may provide a partial explanation for the mislabeling of polysaccharides as crowding agents for nucleic acids. In the present case, a potentially better qualitative interpretation for anticorrelation between enthalpic and entropic changes may be that the more enthalpically stabilized system is also more restrictive with respect to microstate-sampling: e.g., enthalpic binding of the solute to the biomolecule diminishes the overall translational entropy of the solution system.[59]

Based on the thermodynamic evidence, we propose a simple binding model to account qualitatively for the simultaneous enthalpic destabilization ($\Delta\Delta H > 0$) and entropic stabilization ($\Delta(-T\Delta S) < 0$) effects of polysaccharides upon nucleic acid folding (Figure 11). First of all, we expect the abundance of hydroxyl groups on the polysaccharide molecules to be overall attractive to the nucleic acid, in order to have significant impacts on the folding free energy. As a result, the polysaccharide solute will tend to accumulate on the accessible surface area of nucleic acid, enthalpically stabilizing the system at the cost of entropy primarily in the translational degrees of freedom of the bound polysaccharide and solvent reorganiza-

https://doi.org/10.1021/acs.jpcb.1c07852
J. Phys. Chem. B 2021, 125, 13147−13157

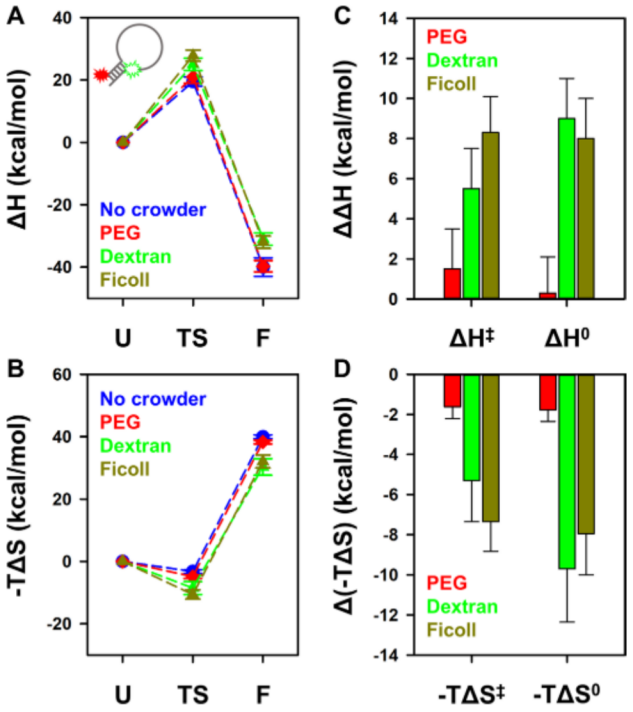

Figure 9. Folding free energy landscapes of the DNA hairpin construct. (A) Enthalpic and (B) entropic contributions along the folding coordinate, with the relative enthalpy/entropy of the unfold state, U conventionally referenced to zero. The corresponding (C) enthalpic and (D) entropic changes by the three crowders at 7.5 wt %. Note that entropic contributions ($-T\Delta S$) to the free energies are estimated for room-temperature conditions (21.0 °C).

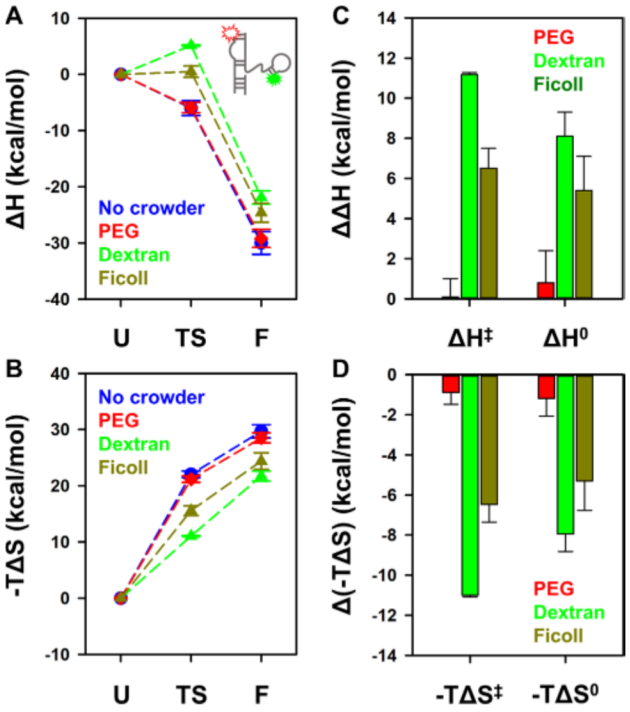

Figure 10. Folding free energy landscapes of the RNA TL-TLR construct. (A) Enthalpic and (B) entropic contributions along the folding coordinate with the relative enthalpy/entropy of the unfold state, U conventionally referenced to zero. The corresponding (C) enthalpic and (D) entropic changes by the three crowders at 7.5 wt %. Note that entropic contributions ($-T\Delta S$) to the free energies are estimated for room-temperature conditions (21.0 °C).

tion. Upon folding, this solvent accessible surface area (SASA) of the nucleic acid decreases, requiring partial expulsion of the associated polysaccharide molecules. The net effect will be a less enthalpically stabilized folded structure ($\Delta\Delta H^0 > 0$) with entropic gain ($\Delta(-T\Delta S^0) < 0$) from freeing the polysaccharide molecules, much as reflected in the thermodynamic results summarized in Figures 9 and 10.

We can take this preferential binding model one step further to interpret the influence of polysaccharide crowders on the folding kinetics. Specifically, the transition state for TL-TLR folding has been previously characterized[29] as a tetraloop and tetraloop receptor in close proximity but with unformed yet "prealigned" hydrogen bonds between the TL and TLR. This is clearly supported by the fact that the majority of the enthalpic stabilization occurs in the second half of the reaction coordinate as the TL-TLR evolves from the TS to the fully folded state (see Figure 10A). As a result, we would expect the majority of changes in SASA to take place as the two folding motifs are brought into contact along the approach from U to TS. By way of support, this would be entirely consistent with the fact that polysaccharide "crowders" primarily influence the temperature dependence of k_{fold}, rather than k_{unfold} (e.g., the slopes in Figure 8). Furthermore, as a result of limited changes in SASA between the TS and F states, the model also correctly predicts the unfolding rate constant (k_{unfold}) to be largely insensitive to differential enthalpic contributions from dextran and Ficoll binding, which is again nicely consistent with the temperature-dependent data in Figure 8. Indeed, the similar impacts of all three crowders revealed in Figure 8B signal the relatively minor role of enthalpic contributions on k_{unfold}. As a result, at least the unfolding kinetics for the tertiary nucleic acid construct appear to be dominated by more purely entropic, excluded volume effects for both PEG and Ficoll/dextran polysaccharide polymers (Figure 4C).

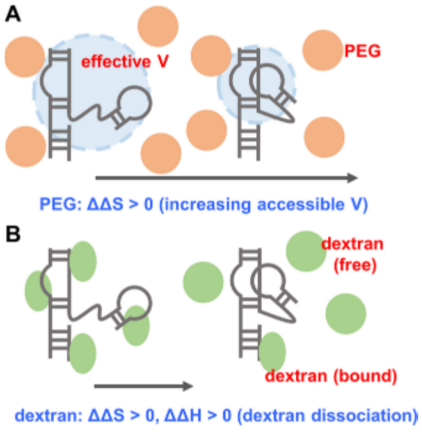

Figure 11. Schematic model for the effects of (A) PEG or (B) dextran on folding of the RNA TL-TLR, highlighting the differential entropic ($\Delta\Delta S > 0$) and enthalpic contributions ($\Delta\Delta H > 0$) due to binding of polysaccharides to the greater solvent accessible surface area (SASA) of the unfolded nucleic acid.

5. SUMMARY AND CONCLUSIONS

Temperature-controlled smFRET confocal microscopy has been used to study the kinetics of solute−biomolecule interactions for common molecular crowding agents, PEG,

https://doi.org/10.1021/acs.jpcb.1c07852
J. Phys. Chem. B 2021, 125, 13147−13157

dextran, and Ficoll, in order to explore/interpret the thermodynamic effects of crowding on nucleic acid secondary (DNA hairpin) and tertiary (RNA TL-TLR) structures. Room-temperature kinetic analysis reveals that PEG promotes nucleic acid folding by simultaneously increasing k_{fold} and decreasing k_{unfold}, qualitatively consistent with predictions from purely entropic crowding effects due to excluded volume interactions. By way of contrast, polysaccharide crowders dextran and Ficoll do not significantly impact either the equilibria or kinetics of nucleic acid folding at room temperature. From temperature-dependent studies, this thermodynamic stabilization at 7.5 wt % PEG is found to be predominantly entropic ($\Delta\Delta S > 0$) with only negligible enthalpic ($\Delta\Delta H \approx 0$) contributions, perfectly consistent with excluded volume models of crowding. By way of contrast, the presence of 7.5 wt % dextran and Ficoll significantly influences both folding enthalpies and entropies, suggesting solute-specific chemical interactions, which we attribute to preferential binding of polysaccharides with the larger SASA of the unfolded nucleic acid construct. The results indicate that the presence of PEG promotes nucleic acid folding predominantly through purely entropic crowding effects without enthalpic contributions. However, these studies also reveal dextran and Ficoll to perturb the folding free energy landscape for nucleic acid folding in more complicated ways, by differential enthalpic contributions to the folded vs unfolded conformations ($\Delta\Delta H \neq 0$) that compete with the purely entropic crowding effects ($\Delta\Delta S > 0$) arising from simple excluded volume models. The results highlight the power of temperature-dependent single-molecule FRET microscopy studies for access to and allowing systematic deconstruction of free energy landscapes into enthalpic and entropic contributions.

AUTHOR INFORMATION

Corresponding Author

David J. Nesbitt − *JILA, National Institute of Standards and Technology, Department of Chemistry, and Department of Physics, University of Colorado, Boulder, Colorado 80309, United States;* orcid.org/0000-0001-5365-1120; Email: djn@jila.colorado.edu

Author

Hsuan-Lei Sung − *JILA, National Institute of Standards and Technology and Department of Chemistry, University of Colorado, Boulder, Colorado 80309, United States*

Complete contact information is available at: https://pubs.acs.org/10.1021/acs.jpcb.1c07852

Notes

The authors declare no competing financial interest.

ACKNOWLEDGMENTS

Initial support for this work has been through the National Science Foundation under grants CHE 1665271 and CHE 2053117 from the Chemical, Structure, Dynamics and Mechanisms-A Program, with recent transition support from the Air Force Office of Scientific Research (FA9550-15-1-0090) and additional funds for development of the confocal apparatus from PHY-1734006 (Physics Frontier Center Program). We would also like to acknowledge early seed contributions by the W. M. Keck Foundation Initiative in RNA Sciences at the University of Colorado, Boulder.

REFERENCES

(1) Fulton, A. B. How Crowded is the Cytoplasm? *Cell* **1982**, *30*, 345−347.
(2) Ellis, R. J. Macromolecular Crowding: Obvious but Underappreciated. *Trends Biochem. Sci.* **2001**, *26*, 597−604.
(3) Minton, A. P. The Influence of Macromolecular Crowding and Macromolecular Confinement on Biochemical Reactions in Physiological Media. *J. Biol. Chem.* **2001**, *276*, 10577−10580.
(4) Gnutt, D.; Ebbinghaus, S. The Macromolecular Crowding Effect − from *in vitro* into the Cell. *Biol. Chem.* **2016**, *397*, 37−44.
(5) Minton, A. P. Excluded Volume as a Determinant of Macromolecular Structure and Reactivity. *Biopolymers* **1981**, *20*, 2093−2120.
(6) Gnutt, D.; Gao, M.; Brylski, O.; Heyden, M.; Ebbinghaus, S. Excluded-Volume Effects in Living Cells. *Am. Ethnol.* **2015**, *54*, 2548−2551.
(7) Cheung, M. S.; Klimov, D.; Thirumalai, D. Molecular Crowding Enhances Native State stability and Refolding Rates of Globular Proteins. *Proc. Natl. Acad. Sci. U. S. A.* **2005**, *102*, 4753.
(8) Zheng, K.-W.; Chen, Z.; Hao, Y.-H.; Tan, Z. Molecular Crowding Creates an Essential Environment for the Formation of Stable G-Quadruplexes in Long Double-Stranded DNA. *Nucleic Acids Res.* **2010**, *38*, 327−338.
(9) Miyoshi, D.; Sugimoto, N. Molecular Crowding Effects on Structure and Stability of DNA. *Biochimie* **2008**, *90*, 1040−1051.
(10) Tokuriki, N.; Kinjo, M.; Negi, S.; Hoshino, M.; Goto, Y.; Urabe, I.; Yomo, T. Protein Folding by the Effects of Macromolecular Crowding. *Protein Sci.* **2004**, *13*, 125−133.
(11) Denos, S.; Dhar, A.; Gruebele, M. Crowding Effects on the Small, Fast-Folding Protein λ_{6-85}. *Faraday Discuss.* **2012**, *157*, 451−462.
(12) Politou, A.; Temussi, P. A. Revisiting a Dogma: the Effect of Volume Exclusion in Molecular Crowding. *Curr. Opin. Struct. Biol.* **2015**, *30*, 1−6.
(13) Blümmel, J.; Perschmann, N.; Aydin, D.; Drinjakovic, J.; Surrey, T.; Lopez-Garcia, M.; Kessler, H.; Spatz, J. P. Protein Repellent Properties of Covalently Attached PEG Coatings on Nanostructured SiO2-Based Interfaces. *Biomaterials* **2007**, *28*, 4739−4747.
(14) Schulz, A.; Woolley, R.; Tabarin, T.; McDonagh, C. Dextran-Coated Silica Nanoparticles for Calcium-Sensing. *Analyst* **2011**, *136*, 1722−1727.
(15) Kilburn, D.; Roh, J. H.; Guo, L.; Briber, R. M.; Woodson, S. A. Molecular Crowding Stabilizes Folded RNA Structure by the Excluded Volume Effect. *J. Am. Chem. Soc.* **2010**, *132*, 8690−8696.
(16) Sasahara, K.; McPhie, P.; Minton, A. P. Effect of Dextran on Protein Stability and Conformation Attributed to Macromolecular Crowding. *J. Mol. Biol.* **2003**, *326*, 1227−1237.
(17) Dupuis, N. F.; Holmstrom, E. D.; Nesbitt, D. J. Molecular-Crowding Effects on Single-Molecule RNA Folding/Unfolding Thermodynamics and Kinetics. *Proc. Natl. Acad. Sci. U. S. A.* **2014**, *111*, 8464.
(18) Minton, A. P. Models for Excluded Volume Interaction between an Unfolded Protein and Rigid Macromolecular Cosolutes: Macromolecular Crowding and Protein Stability Revisited. *Biophys. J.* **2005**, *88*, 971−985.
(19) Christiansen, A.; Wittung-Stafshede, P. Synthetic Crowding Agent Dextran Causes Excluded Volume Interactions Exclusively to Tracer Protein Apoazurin. *FEBS Lett.* **2014**, *588*, 811−814.
(20) Kilburn, D.; Behrouzi, R.; Lee, H.-T.; Sarkar, K.; Briber, R. M.; Woodson, S. A. Entropic Stabilization of Folded RNA in Crowded Solutions Measured by SAXS. *Nucleic Acids Res.* **2016**, *44*, 9452−9461.
(21) Halpin, J. C.; Huang, B.; Sun, M.; Street, T. O. Crowding Activates Heat Shock Protein 90. *J. Biol. Chem.* **2016**, *291*, 6447−6455.
(22) Mukherjee, S.; Waegele, M. M.; Chowdhury, P.; Guo, L.; Gai, F. Effect of Macromolecular Crowding on Protein Folding Dynamics at the Secondary Structure Level. *J. Mol. Biol.* **2009**, *393*, 227−236.

(23) Benton, L. A.; Smith, A. E.; Young, G. B.; Pielak, G. J. Unexpected Effects of Macromolecular Crowding on Protein Stability. *Biochemistry* **2012**, *51*, 9773−9775.
(24) Senske, M.; Törk, L.; Born, B.; Havenith, M.; Herrmann, C.; Ebbinghaus, S. Protein Stabilization by Macromolecular Crowding through Enthalpy Rather Than Entropy. *J. Am. Chem. Soc.* **2014**, *136*, 9036−9041.
(25) Das, N.; Sen, P. Shape-Dependent Macromolecular Crowding on the Thermodynamics and Microsecond Conformational Dynamics of Protein Unfolding Revealed at the Single-Molecule Level. *J. Phys. Chem. B* **2020**, *124*, 5858−5871.
(26) Miyoshi, D.; Nakao, A.; Sugimoto, N. Molecular Crowding Regulates the Structural Switch of the DNA G-Quadruplex. *Biochemistry* **2002**, *41*, 15017−15024.
(27) Knowles, D. B.; LaCroix, A. S.; Deines, N. F.; Shkel, I.; Record, M. T. Separation of Preferential Interaction and Excluded Volume Effects on DNA Duplex and Hairpin Stability. *Proc. Natl. Acad. Sci. U. S. A.* **2011**, *108*, 12699.
(28) Nakano, S.-I.; Miyoshi, D.; Sugimoto, N. Effects of Molecular Crowding on the Structures, Interactions, and Functions of Nucleic Acids. *Chem. Rev.* **2014**, *114*, 2733−2758.
(29) Fiore, J. L.; Holmstrom, E. D.; Nesbitt, D. J. Entropic Origin of Mg^{2+}-Facilitated RNA Folding. *Proc. Natl. Acad. Sci. U. S. A.* **2012**, *109*, 2902.
(30) Sung, H.-L.; Nesbitt, D. J. Novel Heat-Promoted Folding Dynamics of the *yybP-ykoY* Manganese Riboswitch: Kinetic and Thermodynamic Studies at the Single-Molecule Level. *J. Phys. Chem. B* **2019**, *123*, 5412−5422.
(31) Nicholson, D. A.; Sengupta, A.; Sung, H.-L.; Nesbitt, D. J. Amino Acid Stabilization of Nucleic Acid Secondary Structure: Kinetic Insights from Single-Molecule Studies. *J. Phys. Chem. B* **2018**, *122*, 9869−9876.
(32) Sung, H.-L.; Nesbitt, D. J. DNA Hairpin Hybridization under Extreme Pressures: A Single-Molecule FRET Study. *J. Phys. Chem. B* **2020**, *124*, 110−120.
(33) Fiore, J. L.; Kraemer, B.; Koberling, F.; Edmann, R.; Nesbitt, D. J. Enthalpy-Driven RNA Folding: Single-Molecule Thermodynamics of Tetraloop−Receptor Tertiary Interaction. *Biochemistry* **2009**, *48*, 2550−2558.
(34) Aitken, C. E.; Marshall, R. A.; Puglisi, J. D. An Oxygen Scavenging System for Improvement of Dye Stability in Single-Molecule Fluorescence Experiments. *Biophys. J.* **2008**, *94*, 1826−1835.
(35) Sengupta, A.; Sung, H.-L.; Nesbitt, D. J. Amino Acid Specific Effects on RNA Tertiary Interactions: Single-Molecule Kinetic and Thermodynamic Studies. *J. Phys. Chem. B* **2016**, *120*, 10615−10627.
(36) Sung, H.-L.; Nesbitt, D. J. Sequential Folding of the Nickel/Cobalt Riboswitch Is Facilitated by a Conformational Intermediate: Insights from Single-Molecule Kinetics and Thermodynamics. *J. Phys. Chem. B* **2020**, *124*, 7348−7360.
(37) Holmstrom, E. D.; Nesbitt, D. J. Biophysical Insights from Temperature-Dependent Single-Molecule Förster Resonance Energy Transfer. *Annu. Rev. Phys. Chem.* **2016**, *67*, 441−465.
(38) Sung, H.-L.; Nesbitt, D. J. Single-Molecule Kinetic Studies of DNA Hybridization Under Extreme Pressures. *Phys. Chem. Chem. Phys.* **2020**, *22*, 23491−23501.
(39) Fiore, J. L.; Holmstrom, E. D.; Fiegland, L. R.; Hodak, J. H.; Nesbitt, D. J. The Role of Counterion Valence and Size in GAAA Tetraloop−Receptor Docking/Undocking Kinetics. *J. Mol. Biol.* **2012**, *423*, 198−216.
(40) Baltierra-Jasso, L. E.; Morten, M. J.; Laflör, L.; Quinn, S. D.; Magennis, S. W. Crowding-Induced Hybridization of Single DNA Hairpins. *J. Am. Chem. Soc.* **2015**, *137*, 16020−16023.
(41) Patra, S.; Schuabb, V.; Kiesel, I.; Knop, J.-M.; Oliva, R.; Winter, R. Exploring the Effects of Cosolutes and Crowding on the Volumetric and Kinetic Profile of the Conformational Dynamics of a Poly dA Loop DNA Hairpin: a Single-Molecule FRET Study. *Nucleic Acids Res.* **2019**, *47*, 981−996.
(42) Vander Meulen, K. A.; Davis, J. H.; Foster, T. R.; Record, M. T.; Butcher, S. E. Thermodynamics and Folding Pathway of Tetraloop Receptor-Mediated RNA Helical Packing. *J. Mol. Biol.* **2008**, *384*, 702−717.
(43) Sung, H.-L.; Sengupta, A.; Nesbitt, D. Smaller Molecules Crowd Better: Crowder Size Dependence Revealed by Single-Molecule FRET Studies and Depletion Force Modeling Analysis. *J. Chem. Phys.* **2021**, *154*, No. 155101.
(44) Greene, R. F.; Pace, C. N. Urea and Guanidine Hydrochloride Denaturation of Ribonuclease, Lysozyme, α-Chymotrypsin, and *b*-Lactoglobulin. *J. Biol. Chem.* **1974**, *249*, 5388−5393.
(45) Holmstrom, E. D.; Dupuis, N. F.; Nesbitt, D. J. Kinetic and Thermodynamic Origins of Osmolyte-Influenced Nucleic Acid Folding. *J. Phys. Chem. B* **2015**, *119*, 3687−3696.
(46) Yi, Q.; Scalley, M. L.; Simons, K. T.; Gladwin, S. T.; Baker, D. Characterization of the Free Energy Spectrum of Peptostreptococcal Protein L. *Folding Des.* **1997**, *2*, 271−280.
(47) Shelton, V. M.; Sosnick, T. R.; Pan, T. Applicability of Urea in the Thermodynamic Analysis of Secondary and Tertiary RNA Folding. *Biochemistry* **1999**, *38*, 16831−16839.
(48) Auton, M.; Bolen, D. W. Predicting the Energetics of Osmolyte-Induced Protein Folding/Unfolding. *Proc. Natl. Acad. Sci. U. S. A.* **2005**, *102*, 15065.
(49) Wartell, R. M.; Benight, A. S. Thermal Denaturation of DNA Molecules: A Comparison of Theory with Experiment. *Phys. Rep.* **1985**, *126*, 67−107.
(50) Privalov, P. L. Thermodynamics of Protein Folding. *J. Chem. Thermodyn.* **1997**, *29*, 447−474.
(51) Dupuis, N. F.; Holmstrom, E. D.; Nesbitt, D. J. Single-Molecule Kinetics Reveal Cation-Promoted DNA Duplex Formation Through Ordering of Single-Stranded Helices. *Biophys. J.* **2013**, *105*, 756−766.
(52) Zhou, H.-X. Rate Theories for Biologists. *Q. Rev. Biophys.* **2010**, *43*, 219−293.
(53) Szabo, A.; Schulten, K.; Schulten, Z. First Passage Time Approach to Diffusion Controlled Reactions. *J. Chem. Phys.* **1980**, *72*, 4350−4357.
(54) Paudel, B. P.; Rueda, D. Molecular Crowding Accelerates Ribozyme Docking and Catalysis. *J. Am. Chem. Soc.* **2014**, *136*, 16700−16703.
(55) Tyrrell, J.; Weeks, K. M.; Pielak, G. J. Challenge of Mimicking the Influences of the Cellular Environment on RNA Structure by PEG-Induced Macromolecular Crowding. *Biochemistry* **2015**, *54*, 6447−6453.
(56) Sharma, G. S.; Mittal, S.; Singh, L. R. Effect of Dextran 70 on the Thermodynamic and Structural Properties of Proteins. *Int. J. Biol. Macromol.* **2015**, *79*, 86−94.
(57) Malik, A.; Kundu, J.; Mukherjee, S. K.; Chowdhury, P. K. Myoglobin Unfolding in Crowding and Confinement. *J. Phys. Chem. B* **2012**, *116*, 12895−12904.
(58) Dunitz, J. D. Win Some, Lose Some: Enthalpy-Entropy Compensation in Weak Intermolecular Interactions. *Chem. Biol.* **1995**, *2*, 709−712.
(59) Eftink, M. R.; Anusiem, A. C.; Biltonen, R. L. Enthalpy-Entropy Compensation and Heat Capacity Changes for Protein-Ligand Interactions: General Thermodynamic Models and Data for the Binding of Nucleotides to Ribonuclease A. *Biochemistry* **1983**, *22*, 3884−3896.

https://doi.org/10.1021/acs.jpcb.1c07852
J. Phys. Chem. B 2021, 125, 13147−13157